ISSN 1063-7761, Journal of Experimental and Theoretical Physics, 2014, Vol. 119, No. 4, pp. 668–676. © Pleiades Publishing, Inc., 2014.

Dark Energy Model with Generalized Cosmological Horizon[1]

M. Sharif[a],* and A. Jawad[a,b],**

[a] *Department of Mathematics, University of the Punjab Lahore-54590, Pakistan*

[b] *Department of Mathematics, COMSATS Institute of Information Technology, Lahore-54000, Pakistan*

**e-mail: msharif.math@pu.edu.pk*

***e-mail: jawadab181@yahoo.com*

Received March 14, 2014

Abstract—We discuss the evolution of the newly proposed dark-energy model with a generalized event horizon (a generalized form of the holographic dark-energy model with a future event horizon) in the flat and nonflat universes. We consider the interacting scenario of this model with cold dark matter. We use the well-known logarithmic approach to evaluate the equation of state parameter and explore its present values. It is found that this parameter shows phantom crossing in some cases of the generalized event horizon parameters. The ω–ω' plane is also developed for three different cases of the generalized event horizon parameters. The corresponding phase plane provides thawing and freezing regions. Finally, the validity of a generalized second law of thermodynamics is explored which holds in certain ranges of constant parameters.

DOI: 10.1134/S1063776114100100

1. INTRODUCTION

The prediction about the accelerated expansion of the universe is a revolutionary change in modern cosmology. The debate on this topic has been extensive in the last decade in both observational and nonobservational terms. The main focus of this discussion remained on the unknown type of matter, which is assumed to be the major factor of the accelerating universe. A consensus has been developed on dark energy (DE), but its nature is still unclear. In order to resolve this problem, a plethora of work has been done within two main approaches: modification of the gravitational part and of the matter part of the Einstein field equations.

The modification approach in the matter part has led to different dynamical DE models such as the Chaplygin gas [1], holographic [2, 3], agegraphic [4], new agegraphic [5], and scalar field DE models [6–13]. The holographic DE (HDE) model is one of the famous models developed in the framework of quantum gravity. The main motivation behind this model is to achieve consensus about the ambiguous nature of DE. The holographic principle is the origin of this model, according to which the number of degrees of freedom of a physical system should scale with its bounding area rather than its volume [14].

Later on, Cohen et al. [15] developed a relation between ultraviolet (UV) and infrared (IR) cutoffs using the idea of black hole formation in quantum field theory. They argued that the total energy of a system of size L should not exceed the black hole mass of the same size. Using this argument, Hsu [2] developed a model for the density of HDE in the form

$$\rho_\vartheta = 3\lambda^2 m_p^2 L^{-2},$$

where λ is an arbitrary constant and m_p is the reduced Planck mass. Different expressions for the IR cutoff L have been proposed such as Hubble, event, particle horizons [3], Ricci scalar [16] and its generalized form [17]. However, the HDE model with an event horizon has been discussed extensively in the absence [3, 18, 19] and presence [20–22] of interaction with dark matter (DM). These models have also been tested in the framework of different observational schemes and used to develop reliable constraints on different cosmological parameters such as the equation-of-state (EoS) parameter, Hubble parameter, fractional energy densities, etc. [23, 24].

Li [3] explored HDE with a future event horizon using the logarithmic approach and found the present value of the EoS parameter $w_\vartheta = -0.90$. Huang and Li [18] used this approach to examine the evolution of the universe by checking all possible values of the HDE parameter λ and also found that a generalized second law of thermodynamics (GSLT) is preserved for HDE with a future event horizon in a flat as well as closed universe for $\lambda < 1$. They also revealed that HDE with this horizon can cross the phantom region. Jamil et al. [19] investigated the HDE scenario with a varying gravitational constant (G) in both flat and nonflat universes by using the logarithmic approach. They found corrections to the evolution of the EoS parameter in [3] due to variation of G. Lu et al. [24] checked these results within observational schemes and argued that the scenario of HDE with a varying G is compati-

[1] The article is published in the original.

ble with the present observations. They also found the present values of different cosmological parameters in this scenario within a 1σ error range.

Recently, the holographic, agegraphic, and new agegraphic DE models (with event and particle horizons) have been extended to the most general class characterized by dimensionless constant parameters (m, n). The behavior of these models in terms of the EoS parameter, noninteracting and interacting with DM in a flat universe, was investigated in [25]. Cosmological behavior of the universe for a general class of HDE with a particle horizon was explored in [26] within observational schemes in a flat universe. In this paper, we choose an (m, n) type DE model with a generalized cosmological horizon (GCH) (a generalized form of the HDE model with a future event horizon) in flat and nonflat universes. We use the logarithmic approach to evaluate the EoS parameter in the context of interaction with cold DM (CDM). We also discuss the $\omega_\vartheta-\omega'_\vartheta$ plane and the validity of the GSLT.

The rest of the paper is arranged as follows. In Section 2, we investigate the EoS parameter, $\omega_\vartheta-\omega'_\vartheta$, and the GSLT in a flat universe. Section 3 explores the EoS parameter, $\omega_\vartheta-\omega'_\vartheta$, and the GSLT in a nonflat universe. In the Section 4, we summarize our results.

2. FLAT UNIVERSE

In this section, we elaborate a basic cosmological scenario in a flat Friedman–Robertson–Walker (FRW) universe for DE with a GCH. The generalized form of the cosmological horizon is defined as [25, 26]

$$L \equiv R_{GCH} = \frac{1}{a^n(t)}\int_t^\infty a^m(\tilde{t})d\tilde{t}, \tag{1}$$

where $a(t)$ is the cosmic scale factor. We can recover the original HDE with a future event horizon for $m = n = -1$. The time derivative of the above relation yields

$$\dot{R}_{GCH} = -nHR_{GCH} - a^{m-n}, \quad m < 0, \tag{2}$$

where H is the Hubble parameter. The first FRW equation leads to

$$H^2 = \frac{1}{3m_p^2}(\rho_\vartheta + \rho_m), \quad \Omega_\vartheta + \Omega_m = 1, \tag{3}$$

where ρ_ϑ and ρ_m are the respective DE and CDM densities, while

$$\Omega_\vartheta = \frac{\rho_\vartheta}{3m_p^2H^2}, \quad \Omega_m = \frac{\rho_m}{3m_p^2H^2}$$

are the corresponding fractional energy densities. The continuity equations in the interacting case become

$$\dot{\rho}_m + 3H\rho_m = 3u^2H\rho_\vartheta, \tag{4}$$

$$\dot{\rho}_\vartheta + 3H(\rho_\vartheta + p_\vartheta) = -3u^2H\rho_\vartheta, \tag{5}$$

where u^2 is an interaction parameter.

Currently, there are no prior conditions imposed on the possible interactions between DM and DE because neither DE nor DM is understood fundamentally. However, without violating the observational constraints, DE can interact with DM in various fashions by means of energy transfer between each other. The interaction between DE and DM yields a richer cosmological dynamics as compared to noninteracting models and it is possible to solve the cosmic coincidence problem within this framework. However, we cannot describe interaction between these vague nature components from first principles. Therefore, we have to take a specific interaction or set it from phenomenological requirements.

The DE density with a GCH is defined as

$$\rho_\vartheta = 3\lambda^2m_p^2R_{GCH}^{-2}, \tag{6}$$

and its evolutionary form is given by

$$\rho'_\vartheta = 2\rho_\vartheta\left(n + \frac{a^{m-n}\sqrt{\Omega_\vartheta}}{\lambda}\right), \tag{7}$$

where the prime denotes differentiation with respect to $x = \ln a$. By taking the derivative of Eq. (3) with respect to the cosmic time, we obtain

$$\frac{2\dot{H}}{H^2} = -3 + (3(1+u^2) + 2n)\Omega_\vartheta + \frac{2a^{m-n}\Omega_\vartheta^{3/2}}{\lambda}. \tag{8}$$

Differentiating Ω_ϑ with respect to x and using Eqs. (7) and (8) yields

$$\frac{d\Omega_\vartheta}{dx} = \Omega_\vartheta(1-\Omega_\vartheta)\left(3 + 2n + \frac{2a^{m-n}\sqrt{\Omega_\vartheta}}{\lambda} - \frac{3u^2\Omega_\vartheta}{1-\Omega_\vartheta}\right). \tag{9}$$

2.1. Cosmological Implications

We now evaluate the EoS parameter within the logarithmic approach. The DE density is obtained from Eq. (5) in the form

$$\rho_\vartheta = \rho_{\vartheta0}a^{-3(1+\omega_\vartheta+u^2)}, \tag{10}$$

where $\rho_{\vartheta0}$ serves as the current value of the DE density. We use a Taylor series expansion for ρ_ϑ about the present value of $a_0 = 1$ as follows:

$$\begin{aligned}\ln\rho_\vartheta = \ln\rho_\vartheta^0 + \frac{d\ln\rho_\vartheta}{d\ln a}\ln a + \frac{1}{2}\frac{d^2\ln\rho_\vartheta}{d(\ln a)^2}(\ln a)^2 \\ + \frac{1}{6}\frac{d^3\ln\rho_\vartheta}{d(\ln a)^3}(\ln a)^3 + \ldots.\end{aligned} \tag{11}$$

The series is terminated at the second-order derivative because of the small-redshift approximation, i.e., $\ln a = -\ln(1+z) \approx -z$, and it follows from (10) and (11) that

$$\omega_\vartheta = \omega_{\vartheta0} + \omega_{\vartheta1}z, \tag{12}$$

where

$$\omega_{\vartheta 0} = -1-u^2-\frac{1}{3}\frac{d\ln\rho_\vartheta}{d\ln a}, \quad \omega_{\vartheta 1} = \frac{1}{6}\frac{d^2\ln\rho_\vartheta}{d(\ln a)^2}. \quad (13)$$

Here, the derivatives are taken at the present value of a_0. Expressing ρ_ϑ in terms of fractional densities as $\rho_\vartheta = \Omega_\vartheta\rho_m/\Omega_m$, after some calculations, we obtain

$$\frac{d\ln\rho_\vartheta}{d\ln a} = 2n + \frac{2a_0^{m-n}}{\lambda}\sqrt{\Omega_{\vartheta 0}},$$

$$\frac{d^2\ln\rho_\vartheta}{d(\ln a)^2} = \frac{a_0^{m-n}\sqrt{\Omega_{\vartheta 0}}}{\lambda}\Big[2(m-n)+(1-\Omega_{\vartheta 0}) \quad (14)$$

$$\times\left(3+2n+2a_0^{m-n}\lambda^{-1}\sqrt{\Omega_{\vartheta 0}}-\frac{3u^2\Omega_{\vartheta 0}}{1-\Omega_{\vartheta 0}}\right)\Big].$$

Using Eqs. (12)–(14), we obtain the EoS parameter as follows:

$$\omega_\vartheta = -1-u^2-\frac{1}{3}(2n+2a_0^{m-n}\lambda^{-1}\sqrt{\Omega_{\vartheta 0}})$$

$$+\frac{a^{m-n}\sqrt{\Omega_{\vartheta 0}}}{6\lambda}\Big[2(m-n)+(1-\Omega_{\vartheta 0}) \quad (15)$$

$$\times\left(3+2n+2a^{m-n}\lambda^{-1}\sqrt{\Omega_{\vartheta 0}}-\frac{3u^2\Omega_{\vartheta 0}}{1-\Omega_{\vartheta 0}}\right)\Big]z.$$

Using the observational dataset from WMAP + SNIa + BAO + H_0, the best-fit values for the coupling parameter u^2 were presented in [27]. It was also commented there that positive values of this parameter alleviate the cosmological coincidence problem. Here, we take $u^2 = 0.058$ [27] for the interacting case and plot the EoS parameter versus z in the noninteracting case as well (Fig. 1). We choose three different well-settled pairs of the values of m and n by using well-known observational data [26]. It is found that for a given n, the models with $n - m = 1$ are most suitable for discussing the cosmological parameters. For this purpose, we take $n = -1, 0, 1$, which yield $n = -1$, $m = -2$ (Fig. 1a), $n = 0$, $m = -1$ (Fig. 1b), and $n = 1$, $m = 0$ (Fig. 1c). In addition, the case ($n = 0$, $m = -1$) is the most favorable model, also compatible with the ΛCDM model. In Fig. 1a, the present values of the EoS parameter are –0.80 and –0.86 in the noninteracting and interacting cases. The EoS parameter remains in the quintessence region for the near past as well as later time in the noninteracting case, while phantom crossing is observed in the interacting case. In Fig. 1b, the present values of the EoS parameter are approximately –1.46 (in the noninteracting case) and –1.53 (in the interacting case). The universe then exhibits phantom-like behavior in the near past, present, and future cosmic time. However, the large-phantom behavior is observed in the near past compared to the present and later time. In Fig. 1c, we see that the EoS parameter attains the present values in the range –2.14 and –2.20 in the noninteracting and interacting cases. In Fig. 1c, the EoS parameter also exhibits phantom behavior in three different epochs.

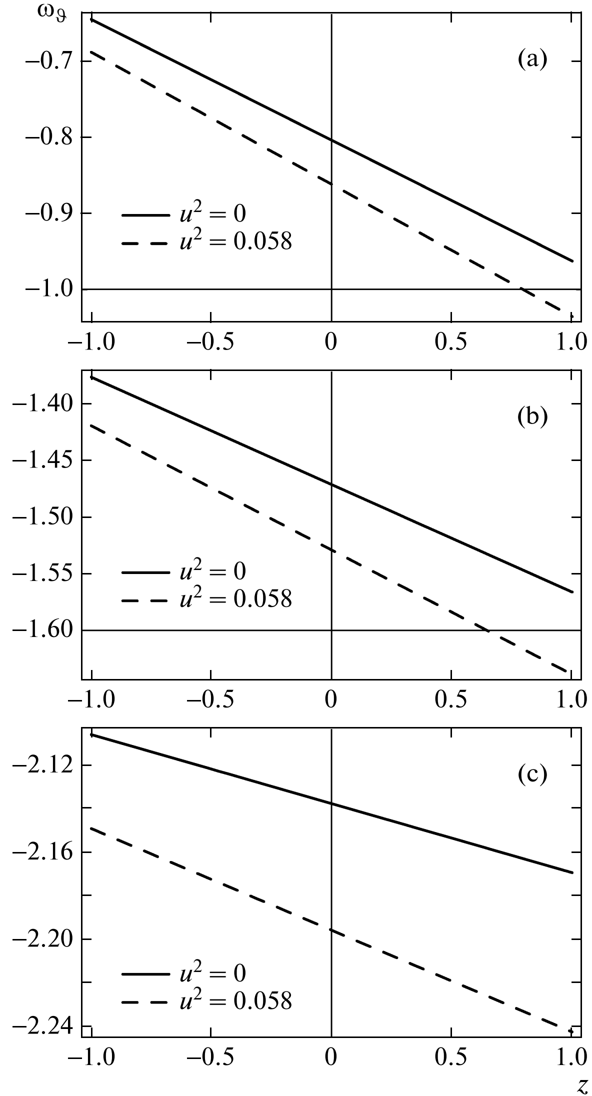

Fig. 1. Plots of ω_ϑ versus z with $u^2 = 0, 0.058$ in the flat case for $n = -1$, $m = -2$ (a), $n = 0$, $m = -1$ (b), and $n = 1$, $m = 0$ (c). We use the present value of the fractional DE density $\Omega_{\vartheta 0} \approx 0.73$ and choose $\lambda = 0.91$.

2.2. ω_ϑ*–*ω'_ϑ *Analysis*

A phenomenon called ω_ϑ–ω'_ϑ for analyzing the behavior of quintessence DE models and the corresponding constraints for these models in the ω_ϑ–ω'_ϑ plane were proposed in [28]. It was pointed out there that the area of this phase plane can be divided into thawing and freezing regions for these models. These regions can be characterized by the values of ω'_ϑ with

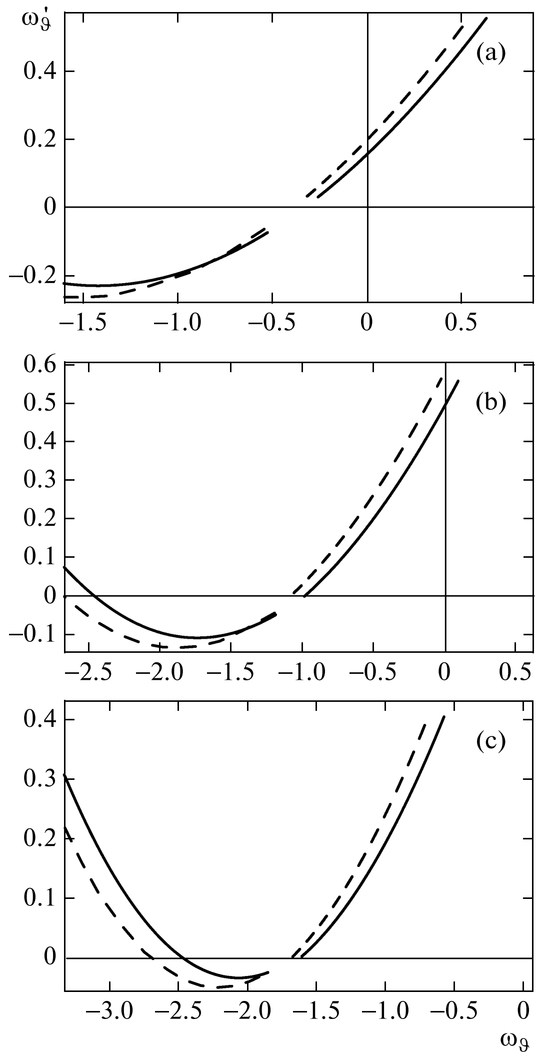

Fig. 2. Plots of ω'_ϑ versus ω_ϑ for $n = -1$, $m = -2$ (a), $n = 0$, $m = -1$ (b), and $n = 1$, $m = 0$ (c). Also, the solid and dashed curves correspond to $u^2 = 0$, 0.058.

respect to ω_ϑ, i.e., $\omega'_\vartheta > 0$, $\omega_\vartheta < 0$ for a thawing region and $\omega'_\vartheta < 0$, $\omega_\vartheta < 0$ for a freezing region. Many authors explored the nature of different DE models (a generalized form of quintessence [29], the phantom [30], quintom [31], polytropic DE [32], and PDE [33, 34] models) using this phenomenon. Here, we analyze the behavior of the DE model with a GCH in a flat universe. The evolution of the EoS parameter turns out to be

$$\omega'_\vartheta = -\frac{a_0^{m-n}\sqrt{\Omega_{\vartheta 0}}}{6\lambda}\Big[2(m-n) + (1-\Omega_{\vartheta 0}) \times \Big(3 + 2n + 2a_0^{m-n}\lambda^{-1}\sqrt{\Omega_{\vartheta 0}} - \frac{3u^2\Omega_{k0}}{1-\Omega_{\vartheta 0}}\Big)\Big]. \tag{16}$$

The plots of ω'_ϑ versus ω_ϑ for three different values of m and n are shown in Fig. 2. The Fig. 2a shows that both curves do not meet the ΛCDM limit ($\omega'_\vartheta = 0$ at $\omega_\vartheta = -1$). However, the present values of ω'_ϑ are approximately equal to -0.15 and -0.20 in the noninteracting and interacting cases with respect to present values of ω_ϑ (as mentioned in Section 2.1). It is also observed that the thawing and freezing regions exist in this plane for both noninteracting and interacting cases. In Fig. 2b, we are able to achieve the ΛCDM limit in the noninteracting case only. In this case, the present values are $\omega'_\vartheta = -0.8, -0.12$ for $u^2 = 0$, 0.058 according to the present values of ω_ϑ. The curve corresponding to $u^2 = 0$ characterizes the thawing region initially, then the freezing region, and finally the thawing region of the $\omega'_\vartheta - \omega_\vartheta$ plane. However, in the interacting case, the curve starts from the thawing region and then goes toward the freezing region. In Fig. 2c, the ΛCDM limit cannot be achieved in both cases of u^2, and the present values of ω'_ϑ with respect to ω_ϑ are -0.02 and -0.04 for the respective values $u^2 = 0$ and 0.058. In this case, both the curves provide thawing as well as freezing regions.

2.3. Generalized Second Law of Thermodynamics

In general relativity, a pioneering relation between thermodynamic quantities and the Einstein field equations has been developed by Jacobson [35]. It is constructed from the entropy–horizon-area proportionality relation by using the first law of thermodynamics $dQ = TdS$, where dQ, T, and dS represent the exchange in energy, temperature, and the entropy change of a given system. Later on, it was argued in [36] that for any spherically symmetric spacetime, the field equations can be written in the form

$$TdS = pdV + dE, \tag{17}$$

where T, S, E, and p are the basic entities of a thermodynamical system: the temperature, entropy, internal energy, and pressure.

The GSLT is originated from the black hole mechanics, where the second law states that the total area of the outer boundary of a family of black holes cannot decrease even as they swallow or collide with each other. In the case of a thermodynamical system, the entropy plays the role of area and the GSLT states that the sum of the entropy of surrounding constituents of matter and the entropy of the black hole itself would increase [37]. Here, we are interested in discussing the GSLT for a system containing the interaction of DE and CDM on the GCH. For this purpose, we need the quantities

$$V = \frac{4\pi L^3}{3}, \quad T = \frac{1}{2\pi L}, \qquad E = \frac{4\pi L^3}{3}\rho, \quad S_H = \pi L^2. \tag{18}$$

The time rate of Eq. (17) for DE and CDM yields

$$\dot{S}_\vartheta = \frac{p_\vartheta \dot{V} + \dot{E}_\vartheta}{T}, \quad \dot{S}_m = \frac{p_m \dot{V} + \dot{E}_m}{T}. \tag{19}$$

We check the GSLT for a system in equilibrium. Using Eqs. (4), (5), (18), and (19), we can obtain the final form of the GSLT:

$$T\dot{S}_{\text{total}} = -\frac{3\lambda^2}{2\Omega_\vartheta}(1 + \omega_\vartheta\Omega_\vartheta)\left(\frac{(n+1)\lambda}{\sqrt{\Omega_\vartheta}} + a^{m-n}\right) - \left(\frac{n\lambda}{\sqrt{\Omega_\vartheta}} + a^{m-n}\right). \tag{20}$$

At present time, this expression becomes

$$T\dot{S}_{\text{total}} = -\frac{3\lambda^2}{2\Omega_{\vartheta 0}}\left\{1 + \left[-1 - u^2 - \frac{1}{3}\left(2n + \frac{2a_0^{m-n}}{\lambda}\sqrt{\Omega_{\vartheta 0}}\right)\Omega_{\vartheta 0}\right]\right\} \times \left(\frac{(n+1)\lambda}{\sqrt{\Omega_{\vartheta 0}}} + a_0^{m-n}\right) - \left(\frac{n\lambda}{\sqrt{\Omega_{\vartheta 0}}} + a_0^{m-n}\right). \tag{21}$$

Here, T does not violate the validity of the GSLT. We analyze the validity of the GSLT by plotting $T\dot{S}_{\text{total}}$ in the well-established range $0.3 \le \lambda \le 1$ at the present cosmic time in Fig. 3. Also, we use observationally settled values of m, n, and u^2. In Fig. 3a, we can observe that the GSLT violates its validity in the range $0.3 \le \lambda < 0.88$ and preserves its validity for $0.88 \le \lambda \le 1$. In Fig. 3b, the GSLT does not remain valid for both noninteracting and interacting cases. It is observed that the GSLT remains valid for $0.82 \le \lambda \le 1$ in the noninteracting case and for $0.78 \le \lambda \le 1$ in the interacting case (Fig. 3c).

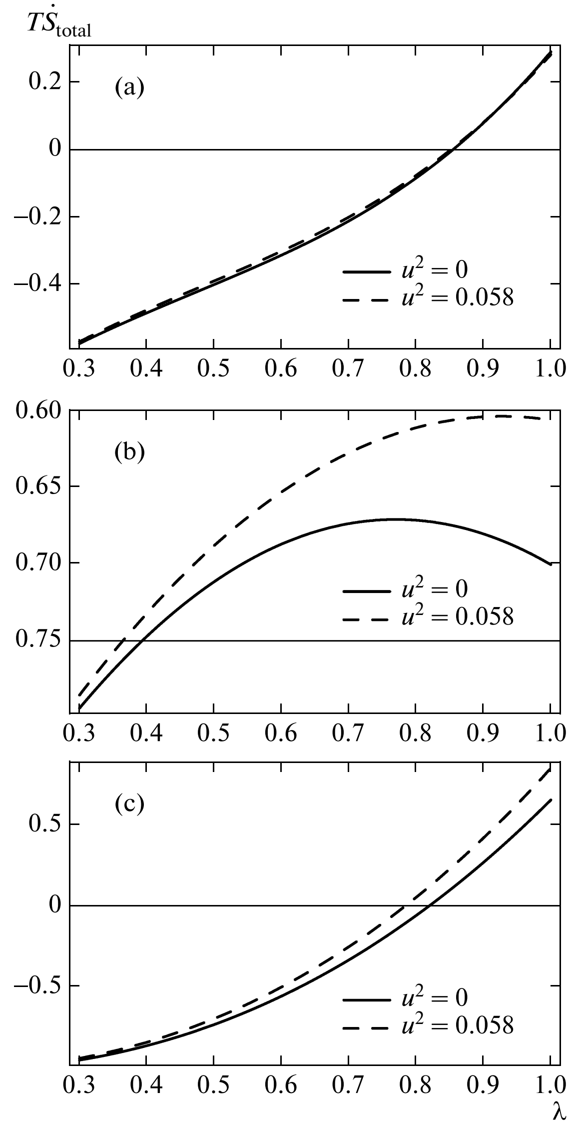

Fig. 3. Plots of $T\dot{S}_{\text{total}}$ versus λ, at the present time, for $n = -1$, $m = -2$ (a), $n = 0$, $m = -1$ (b), and $n = 1$, $m = 0$ (c). Also, the solid and dashed curves correspond to $u^2 = 0$, 0.058.

3. NONFLAT UNIVERSE

In this section, we repeat the above analysis for a nonflat universe. We define the corresponding generalized form of the cosmological horizon as

$$L = a^{-n}\sin y, \quad y = a^n R_{GCH}, \tag{22}$$

whose time derivative takes the form

$$\dot{L} = -nHL - a^{m-n}\cos y. \tag{23}$$

The first FRW equation in a nonflat universe becomes

$$H^2 + \frac{k}{a^2} = \frac{1}{3m_p^2}(\rho_m + \rho_\vartheta), \quad \Omega_\vartheta + \Omega_m = 1 + \Omega_k, \tag{24}$$

where $\Omega_k = k/a^2H^2$ is the fractional energy density. The derivative of Eq. (24) with respect to the

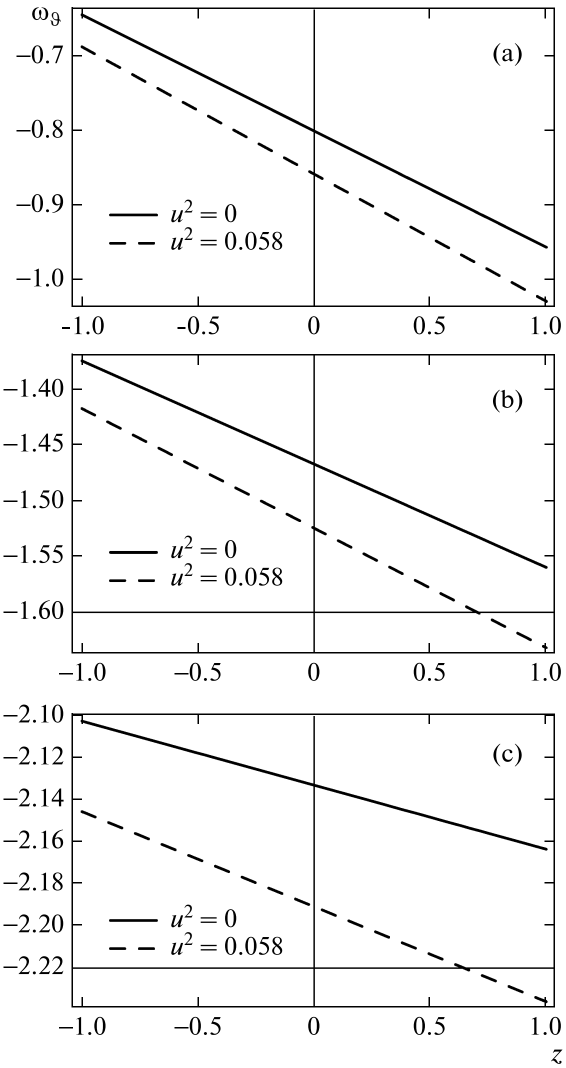

Fig. 4. Plots of ω_ϑ versus z with $u^2 = 0, 0.058$ in the nonflat case for $n = -1$, $m = -2$ (a), $n = 0$, $m = -1$ (b), and $n = 1$, $m = 0$ (c). We use the present value of the fractional DE density $\Omega_{\vartheta 0} \approx 0.73$ and choose $\lambda = 0.91$.

cosmic time yields

$$\frac{2\dot{H}}{H^2} = -3 - \Omega_k + (3(1+u^2) + 2n)\Omega_\vartheta + \frac{2a^{m-n}\Omega_\vartheta^{3/2}}{\lambda}\cos y. \tag{25}$$

The corresponding evolution of the DE density turns out to be

$$\rho'_\vartheta = 2\rho_\vartheta\left(n + \frac{a^{m-n}\sqrt{\Omega_\vartheta}}{\lambda}\cos y\right). \tag{26}$$

Equations (25) and (26) yield

$$\begin{aligned}\frac{d\Omega_\vartheta}{dx} &= \Omega_\vartheta(1 - \Omega_\vartheta + \Omega_k) \\ &\times\left[2n(1-\Omega_k) + \frac{2a^{m-n}\sqrt{\Omega_\vartheta}}{\lambda}(1-\Omega_k)\cos y + 3 - \frac{3u^2\Omega_\vartheta}{1-\Omega_\vartheta+\Omega_k} - \frac{2\Omega_k}{1-\Omega_\Lambda+\Omega_k}\right], \\ \frac{d\Omega_k}{dx} &= -\Omega_k\left[-1 - \Omega_k + (3(1+u^2)+2n)\Omega_\vartheta + \frac{2a^{m-n}\Omega_\vartheta^{3/2}}{\lambda}\cos y\right].\end{aligned} \tag{27}$$

In the nonflat universe, the derivatives required for the EoS parameter at the present time take the form

$$\begin{aligned}\frac{d\ln\rho_\vartheta}{d\ln a} &= 2n + \frac{2}{\lambda}\sqrt{\Omega_{\vartheta 0}}, \\ \frac{d^2\ln\rho_\vartheta}{d(\ln a)^2} &= \frac{\sqrt{\Omega_{\vartheta 0}}}{\lambda}\Big[2m - 2n\Omega_{\vartheta 0} - 3u^2\Omega_{\vartheta 0} \\ &+ 3\left(1 - \Omega_{\vartheta 0} + \frac{\Omega_{k0}}{3}\right) + 2\lambda^{-1}\sqrt{\Omega_{\vartheta 0}}(1-\Omega_{\vartheta 0})\Big] \\ &+ 2(0.0123)^2 + \Omega_{\vartheta 0}\lambda^{-2}.\end{aligned} \tag{28}$$

Here, we have used the current values

$$\sin y = \frac{\lambda\sqrt{\Omega_{k0}}}{\sqrt{\Omega_{\vartheta 0}}} = 0.0123,$$

$$\cos y = \sqrt{\frac{\Omega_{\vartheta 0} - \lambda^2\Omega_{k0}}{\Omega_{\vartheta 0}}} = 0.999 \approx 1,$$

while the values of other constant parameters are the same as in the preceding section. Inserting the above derivatives in Eq. (13), we obtain the EoS parameter as

$$\begin{aligned}\omega_\vartheta &= -1 - \frac{1}{3}(2n + 2\lambda^{-1}\sqrt{\Omega_{\vartheta 0}}) \\ &- [\sqrt{\Omega_{\vartheta 0}}(6\lambda)^{-1}(2m - 2n - 3u^2\Omega_{\vartheta 0} \\ &+ 3(1 - \Omega_{\vartheta 0} + 3^{-1}\Omega_k) + 2\lambda^{-1}\sqrt{\Omega_\vartheta}(1-\Omega_\vartheta)) \\ &+ 2(0.013)^2\Omega_{\vartheta 0}\lambda^{-2}]z.\end{aligned} \tag{29}$$

The plot of the above parameter is shown in Fig. 4 versus the same parameters as in Section 2. The present values $\omega_{\vartheta 0}$ are approximately equal to -0.82 and -0.88 in the noninteracting and interacting cases, as shown in Fig. 4a. In the interacting case, the EoS parameter lies in the quintessence for the near past, present, and later epoch. However, the EoS parameter behaves like a phantom in the near past; after a short interval of time, it crosses the vacuum era and then goes toward the quintessence region in the noninteracting case. In Fig. 4b, the present values of the EoS parameter are -1.48 and -1.54 corresponding to the noninteracting and interacting cases. However, the universe behaves like a phantom in this model in all epochs. In Fig. 4c, the present values of ω_ϑ correspond to -2.13 and -2.19 for the noninteracting and interacting cases. However, the universe also remains in the phantom region but attains more negative values as compared to preceding case.

For $\omega_\vartheta - \omega'_\vartheta$, we differentiate Eq. (29) as

$$\omega'_\vartheta = -[\sqrt{\Omega_{\vartheta 0}}(6\lambda)^{-1}(2m - 2n - 3u^2\Omega_{\vartheta 0}3 + (1 - \Omega_{\vartheta 0} + 3^{-1}\Omega_k) + 2\lambda^{-1}\sqrt{\Omega_\vartheta}(1 - \Omega_\vartheta)) + 2(0.013)^2\Omega_{\vartheta 0}\lambda^{-2}]. \tag{30}$$

The $\omega_\vartheta - \omega'_\vartheta$ plane is shown in Fig. 5 with the same constant parameters. The present values of ω'_ϑ are -0.15 and -0.20 (Fig. 5a), -0.9 and -0.14 (Fig. 5b), and -0.03 and -0.05 (Fig. 5c) for the noninteracting and interacting cases, respectively. The ΛCDM limit is only attained in the noninteracting case in Fig. 5b. In addition, thawing and freezing regions exist in all cases.

In this context, the expression of the GSLT turns out to be

$$T\dot{S}_{\text{total}} = -\frac{3\lambda^2}{2\Omega_\vartheta}(1 + \Omega_k + \omega_\vartheta\Omega_\vartheta)\left(\frac{(n+1)\lambda}{\sqrt{\Omega_\vartheta}} + a^{m-n}\cos y\right) - \left(\frac{n\lambda}{\sqrt{\Omega_\vartheta}} + a^{m-n}\cos y\right). \tag{31}$$

We plot it at the present state versus λ in Fig. 6. We observe that the GSLT is valid for $0.86 \le \lambda \le 1$ (Fig. 6a in the noninteracting and interacting cases), $0.80 \le \lambda \le 1$ (Fig. 6b in the noninteracting case), and $0.76 \le \lambda \le 1$ (Fig. 6c in the interacting case).

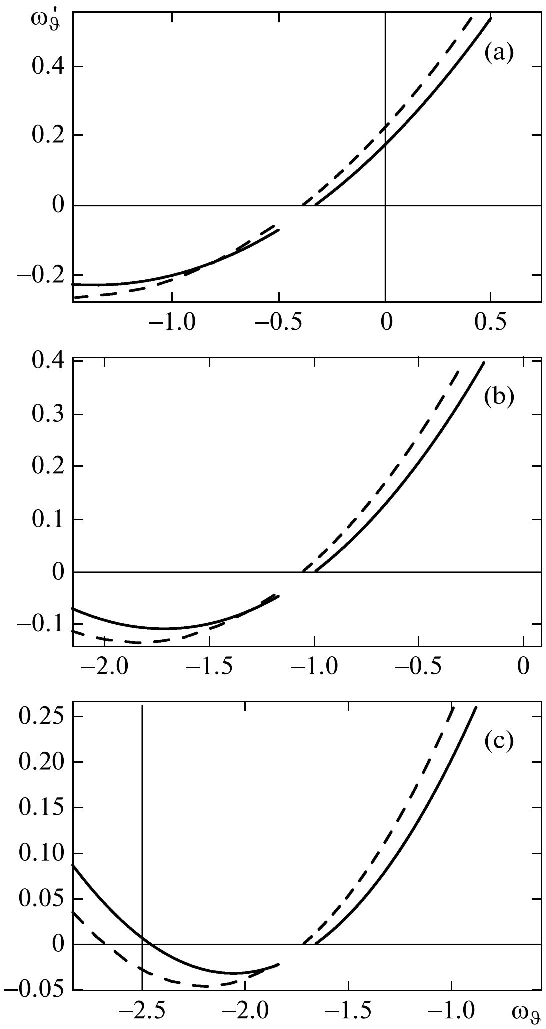

Fig. 5. Plots of ω'_ϑ versus ω_ϑ in a nonflat universe for $n = -1$, $m = -2$ (a), $n = 0$, $m = -1$ (b), and $n = 1$, $m = 0$ (c). Also, the solid and dashed curves correspond to $u^2 = 0$, 0.058.

4. CONCLUDING REMARKS

The purpose of this work is to study the cosmic acceleration within the interacting DE model with CDM in flat and nonflat universes. We have explored the EoS parameter in terms of different cosmological and constant parameters in the logarithmic approach with the Taylor series expansion up to the second order. The reason is that we would like to make corrections in the behavior of the EoS parameter and reduce the deficiencies. In the discussion of this parameter, three constant parameters play the crucial role, i.e., GCH parameters (m, n) and the interaction parameter u^2. We have observed the behavior of the EoS parameter with respect to m, n, u^2 and obtained some constraints on the present values of ω_ϑ. We have chosen the observation-ally settled values of constant parameter like m, n [26], and u^2 [27].

In the flat case (Fig. 1), the approximated present values of ω_ϑ in the respective noninteracting and interacting cases are -0.80, -0.86 (Fig. 1a), -1.46, -1.53 (Fig. 1b), and -2.14, -2.20 (Fig. 1c). We note that the phantom behavior cannot be achieved in the noninteracting case in the left plot. However, phantom crossing was observed in the interacting case, i.e., the EoS parameter starts from the phantom region in the near past and goes toward the quintessence region by evolving the vacuum region. In Figs. 1b, 1c, totally phantomlike behavior has been observed, but a greater phantom effect has been observed in Fig. 1c. In the nonflat case, the approximated present values of the EoS parameter in the noninteracting and interacting cases are $\omega_{\vartheta 0} = -0.82$ and -0.88, $\omega_{\vartheta 0} = -1.48$ and -1.54, and $\omega_{\vartheta 0} = -2.13$ and -2.19, as shown in Figs. 4a, 4b and 4c. However, the behavior of the EoS parameter is similar to that in the flat case.

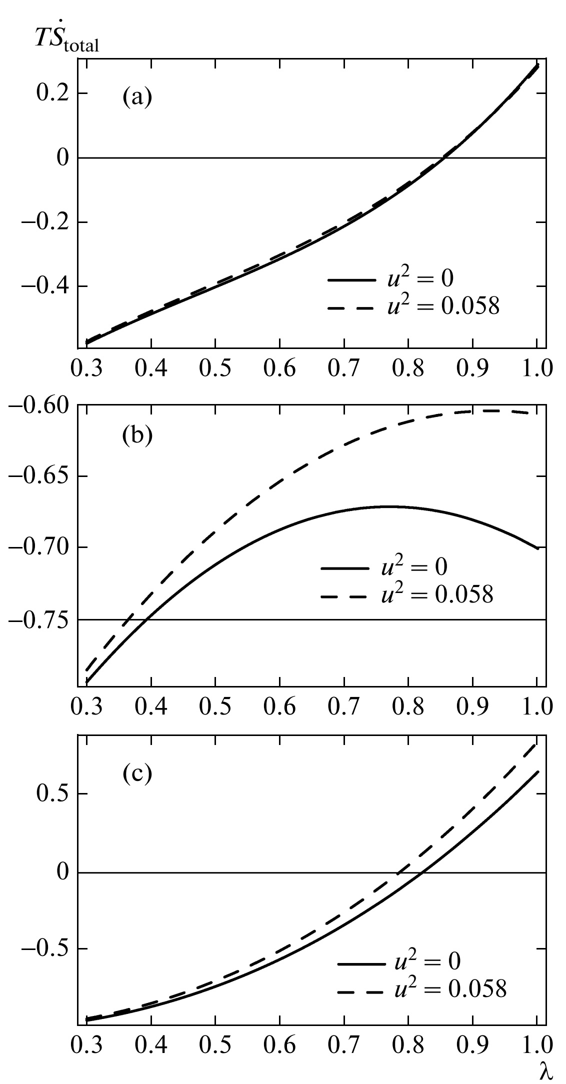

Fig. 6. Plots of $T\dot{S}_{\text{total}}$ versus ω_ϑ, at the present time, for $n = -1$, $m = -2$ (a), $n = 0$, $m = -1$ (b), and $n = 1$, $m = 0$ (c) in a nonflat universe. Also, the solid and dashed curves correspond to $u^2 = 0, 0.058$.

By taking different combination of observational schemes, Ade et al. [38] have put the following constraints on the EoS parameter:

$$\omega_\vartheta = -1.13^{+0.24}_{-0.25} \quad \text{(Planck + WP + BAO)},$$

$$\omega_\vartheta = -1.09 \pm 0.17 \quad \text{(Planck + WP + Union 2.1)},$$

$$\omega_\vartheta = -1.13^{+0.13}_{-0.14} \quad \text{(Planck + WP + SNLS)},$$

$$\omega_\vartheta = -1.24^{+0.18}_{-0.419} \quad \text{(Planck + WP + } H_0\text{)}$$

at 95% confidence level. It can be seen from the *a* and *b* panels in Figs. 1 and 4 that the EoS parameter approximately represents the above values for all cases of the interaction parameter, which shows consistency of our results. We also observe that as n increases, this parameter deviates from -1 for chosen pairs of (n, m).

We have also explored $\omega_\vartheta - \omega'_\vartheta$ in both flat and nonflat universes and found coincidence of the DE model with the ΛCDM model. The ΛCDM limit is achieved only in the noninteracting scenario for $n = 0$, $m = -1$ in flat as well as nonflat universes (Figs. 2b and 5b). The present values of ω'_ϑ with respect to ω_ϑ are also obtained. Finally, we have explored the GSLT in this scenario at the present epoch with respect to λ for three different choices of n and m by setting the well-established values of the remaining constant parameters. It is found that the GSLT remains valid in the specific ranges of λ.

We thank the Higher Education Commission, Islamabad, Pakistan, for its financial support through the Indigenous Ph.D. 5000 Fellowship Program Batch-VII.

REFERENCES

1. A. Y. Kamenshchik, U. Moschella, and V. Pasquier, Phys. Lett. B **511**, 265 (2001); M. C. Bento, O. Bertolami, and A. A. Sen, Phys. Rev. D: Part. Fields **66**, 043507 (2002); X. Zhang, F. Q. Wu, and J. Zhang, J. Cosmol. Astropart. Phys., issue 01, 003 (2006).
2. S. D. H. Hsu, Phys. Lett. B **594**, 13 (2004).
3. M. Li, Phys. Lett. B **603**, 1 (2004).
4. R. G. Cai, Phys. Lett. B **657**, 228 (2007).
5. H. Wei and R. G. Cai, Phys. Lett. B **660**, 113 (2008).
6. B. Ratra and P. J. E. Peebles, Phys. Rev. D: Part. Fields **37**, 3406 (1988).
7. A. A. Starobinsky, JETP Lett. **68** (10), 757 (1998).
8. D. Huterer and M. S. Turner, Phys. Rev. D: Part. Fields **60**, 081301 (1999).
9. T. Nakamura and T. Chiba, Mon. Not. R. Astron. Soc. **306**, 696 (1999).
10. C. Armendariz-Picon, T. Damour, and V. Mukhanov, Phys. Lett. B **458**, 209 (1999); T. Chiba, T. Okabe, and M. Yamaguchi, Phys. Rev. D: Part. Fields **62**, 023511 (2000).
11. R. R. Caldwell, Phys. Lett. B **545**, 23 (2002); S. M. Carroll, M. Hoffman, and M. Trodden, Phys. Rev. D: Part. Fields **68**, 023509 (2003).
12. B. Feng, X. L. Wang, and X. M. Zhang, Phys. Lett. B **607**, 35 (2005).
13. T. Padmanabhan, Phys. Rev. D: Part. Fields **66**, 021301 (2002); J. S. Bagla, H. K. Jassal, and T. Padmanabhan, Phys. Rev. D: Part. Fields **67**, 063504 (2003).
14. L. Susskind, J. Math. Phys. **36**, 6377 (1995).
15. A. Cohen, D. Kaplan, and A. Nelson, Phys. Rev. Lett. **82**, 4971 (1999).
16. C. Gao, X. Chen, and Y. G. Shen, Phys. Rev. D: Part., Fields, Gravitation, Cosmol. **79**, 043511 (2009).
17. M. Sharif and A. Jawad, Eur. Phys. J. C **72**, 2097 (2012); L. Granda and A. Oliveros, Phys. Lett. B **669**, 275 (2008); S. Chen and J. Jing, Phys. Lett. B **679**, 144 (2009); L. Xua, J. Lu, and W. Li, Eur. Phys. J. C **64**, 89

(2009); J. Lu, Y. Wang, Y. Wu, and T. Wang, Eur. Phys. J. C **71**, 1800 (2011).

18. Q. G. Huang and M. Li, J. Cosmol. Astropart. Phys., issue 04, 013 (2004).
19. M. Jamil, E. N. Saridakis, and M. R. Setare, Phys. Lett. B **679**, 172 (2009).
20. M. R. Setare, J. Cosmol. Astropart. Phys. **1**, 023 (2007).
21. M. Sharif and A. Jawad, Eur. Phys. J. C **72**, 1901 (2012).
22. M. Sharif and A. Jawad, Astrophys. Space Sci. **337**, 789 (2012).
23. Q. G. Huang and Y. G. Gong, J. Cosmol. Astropart. Phys., issue 08, 006 (2004); S. B. Wang, E. Abdalla, and R. K. Su, Phys. Lett. B **609**, 200 (2005); X. Zhang and F. Q. Wu, Phys. Rev. D: Part., Fields, Gravitation, Cosmol. **72**, 043524 (2005); C. Feng, B. Wang, Y. Gong, and R.-K. Su, J. Cosmol. Astropart. Phys., issue 09, 005 (2007).
24. J. Lu, E. N. Saridakis, M. R. Setare, and L. Xu, J. Cosmol. Astropart. Phys., issue 03, 031 (2010).
25. Y. Ling and W. J. Pan, Mod. Phys. Lett. A **28**, 1350128 (2013).
26. Z. P. Huang and Y. L. Wu, J. Cosmol. Astropart. Phys., issue 07, 035 (2012).
27. J. H. He, B. Wang, and E. Abdalla, Phys. Rev. D: Part., Fields, Gravitation, Cosmol. **83**, 063515 (2011).
28. R. R. Caldwell and E. V. Linder, Phys. Rev. Lett. **95**, 141301 (2005).
29. R. J. Scherrer, Phys. Rev. D: Part., Fields, Gravitation, Cosmol. **73**, 043502 (2006).
30. T. Chiba, Phys. Rev. D: Part., Fields, Gravitation, Cosmol. **73**, 063501 (2006).
31. Z. K. Guo, Y. S. Piao, X. M. Zhang, and Y. Z. Zhang, Phys. Rev. D: Part., Fields, Gravitation, Cosmol. **74**, 127304 (2006).
32. M. Malekjani and A. Khodam-Mohammadi, Int. J. Theor. Phys. **51**, 3141 (2012).
33. M. Sharif and A. Jawad, Eur. Phys. J. C **73**, 2382 (2013).
34. M. Sharif and A. Jawad, Eur. Phys. J. C **73**, 2600 (2013).
35. T. Jacobson, Phys. Rev. Lett. **75**, 1260 (1995).
36. T. Padmanabhan, Classical Quantum Gravity **19**, 5387 (2002).
37. J. D. Bekenstein, Phys. Rev. D: Part. Fields **7**, 2333 (1973).
38. P. A. R. Ade, N. Aghanim, C. Armitage-Caplan, M. Arnaud, M. Ashdown, F. Atrio-Barandela, J. Aumont, C. Baccigalupi, A. J. Banday, R. B. Barreiro, J. G. Bartlett, E. Battaner, K. Benabed, A. Benoît, A. Benoit-Lévy, J.-P. Bernard, M. Bersanelli, P. Bielewicz, J. Bobin, J. J. Bock, A. Bonaldi, J. R. Bond, J. Borrill, F. R. Bouchet, M. Bridges, M. Bucher, C. Burigana, R. C. Butler, E. Calabrese, B. Cappellini, J.-F. Cardoso, A. Catalano, A. Challinor, A. Chamballu, R.-R. Chary, X. Chen, H. C. Chiang, L.-Y. Chiang, P. R. Christensen, S. Church, D. L. Clements, S. Colombi, L. P. L. Colombo, F. Couchot, A. Coulais, B. P. Crill, A. Curto, F. Cuttaia, L. Danese, R. D. Davies, R. J. Davis, P. de Bernardis, A. de Rosa, G. de Zotti, J. Delabrouille, J.-M. Delouis, F.-X. Désert, C. Dickinson, J. M. Diego, K. Dolag, H. Dole, S. Donzelli, O. Doŕ, M. Douspis, J. Dunkley, X. Dupac, G. Efstathiou, F. Elsner, T. A. Enßlin, H. K. Eriksen, F. Finelli, O. Forni, M. Frailis, A. A. Fraisse, E. Franceschi, T. C. Gaier, S. Galeotta, S. Galli, K. Ganga, M. Giard, G. Giardino, Y. Giraud-Héraud, E. Gjerløw, J. Gonz'lez-Nuevo, K. M. Górski, S. Gratton, A. Gregorio, A. Gruppuso, J. E. Gudmundsson, J. Haissinski, J. Hamann, F. K. Hansen, D. Hanson, D. Harrison, S. Henrot-Versillé, C. Hernández-Monteagudo, D. Herranz, S. R. Hildebrandt, E. Hivon, M. Hobson, W. A. Holmes, A. Hornstrup, Z. Hou, W. Hovest, K. M. Huffenberger, A. H. Jaffe, T. R. Jaffe, J. Jewell, W. C. Jones, M. Juvela, E. Keihänen, R. Keskitalo, T. S. Kisner, R. Kneissl, J. Knoche, L. Knox, M. Kunz, H. Kurki-Suonio, G. Lagache, A. Lähteenmäki, J.-M. Lamarre, A. Lasenby, M. Lattanzi, R. J. Laureijs, C. R. Lawrence, S. Leach, J. P. Leahy, R. Leonardi, J. León-Tavares, J. Lesgourgues, A. Lewis, M. Liguori, P. B. Lilje, M. Linden-Vørnle, M. López-Caniego, P. M. Lubin, J. F. Macías-Pérez, B. Maffei, D. Maino, N. Mandolesi, M. Maris, D. J. Marshall, P. G. Martin, E. Martínez-González, S. Masi, M. Massardi, S. Matarrese, F. Matthai, P. Mazzotta, P. R. Meinhold, A. Melchiorri, J.-B. Melin, L. Mendes, E. Menegoni, A. Mennella, M. Migliaccio, M. Millea, S. Mitra, M.-A. Miville-Deschênes, A. Moneti, L. Montier, G. Morgante, D. Mortlock, A. Moss, D. Munshi, J. A. Murphy, P. Naselsky, F. Nati, P. Natoli, C. B. Netterfield, H. U. Nørgaard-Nielsen, F. Noviello, D. Novikov, I. Novikov, I. J. O'Dwyer, S. Osborne, C. A. Oxborrow, F. Paci, L. Pagano, F. Pajot, D. Paoletti, B. Partridge, F. Pasian, G. Patanchon, D. Pearson, T. J. Pearson, H. V. Peiris, O. Perdereau, L. Perotto, F. Perrotta, V. Pettorino, F. Piacentini, M. Piat, E. Pierpaoli, D. Pietrobon, S. Plaszczynski, P. Platania, E. Pointecouteau, G. Polenta, N. Ponthieu, L. Popa, T. Poutanen, G. W. Pratt, G. Prézeau, S. Prunet, J.-L. Puget, J. P. Rachen, W. T. Reach, R. Rebolo, M. Reinecke, M. Remazeilles, C. Renault, S. Ricciardi, T. Riller, I. Ristorcelli, G. Rocha, C. Rosset, G. Roudier, M. Rowan-Robinson, J. A. Rubiño-Martín, B. Rusholme, M. Sandri, D. Santos, M. Savelainen, G. Savini, D. Scott, M. D. Seiffert, E. P. S. Shellard, L. D. Spencer, J.-L. Starck, V. Stolyarov, R. Stompor, R. Sudiwala, R. Sunyaev, F. Sureau, D. Sutton, A.-S. Suur-Uski, J.-F. Sygnet, J. A. Tauber, D. Tavagnacco, L. Terenzi, L. Toffolatti, M. Tomasi, M. Tristram, M. Tucci, J. Tuovinen, M. Türler, G. Umana, L. Valenziano, J. Valiviita, B. Van Tent, P. Vielva, F. Villa, N. Vittorio, L. A. Wade, B. D. Wandelt, I. K. Wehus, M. White, S. D. M. White, A. Wilkinson, D. Yvon, A. Zacchei, and A. Zonca [Planck Collab.], arXiv:1303.5076.